

TEMPERATURE DISTURBANCE IN A GEOTHERMAL  
BOREHOLE SYSTEM

A THESIS

Presented to  
The Faculty of the Division of  
Graduate Studies

By  
Ching-hua Chen

In Partial Fulfillment  
of the Requirements for the Degree  
Master of Science in Geophysical Sciences

Georgia Institute of Technology  
October, 1975

TEMPERATURE DISTURBANCE IN A GEOTHERMAL  
BOREHOLE SYSTEM

Approved:

Robert P. Lowell, Chairman

Leland T. Long

C. O. Pollard, Jr.

Date approved by Chairman: 12/1/75

## ACKNOWLEDGMENTS

It is with pleasure that I acknowledge the assistance and guidance of my advisor, Dr. R. P. Lowell, who not only suggested the topic of my research, but also provided the necessary motivation to complete the investigation. I would also like to extend my thanks to my reading committee, Drs. L. T. Long and C. O. Pollard, Jr., for their helpful suggestions and comments.

I would like to thank the National Energy Authority, Reykjavik, Iceland for providing the temperature data used in Figure 15.

Finally, I would especially like to thank my parents for their patience, love and support during this endeavor.

## TABLE OF CONTENTS

	Page
ACKNOWLEDGMENTS. . . . .	ii
LIST OF SYMBOLS AND UNITS. . . . .	iv
LIST OF TABLES . . . . .	vi
LIST OF ILLUSTRATIONS. . . . .	vii
SUMMARY. . . . .	viii
Chapter	
I. INTRODUCTION AND RELATED WORK. . . . .	1
II. MODELING OF THE CIRCULATING BOREHOLE SYSTEMS . . . . .	4
Description of the Basic Model	
The Basic Equations	
Further Approximation to the Outlet Temperature and the Bottom-Hole Temperature	
The Model with Non-Linear Geothermal Gradients	
The Model with Fluid Losses	
III. RELAXATION OF DRILLING DISTURBANCE . . . . .	31
Temperature Distribution of the Fluids in a Fracture	
Temperature Disturbance Resulting from the Drilling Fluid Loss	
Relaxation after the Drilling Ceases	
Application of the Fluid-Loss Model	
IV. CONCLUSIONS. . . . .	47
BIBLIOGRAPHY . . . . .	49

## LIST OF SYMBOLS AND UNITS

a	Thermal diffusivity of rock, $m^2/sec$
c	Specific heat of rock, $kJ/kg-^{\circ}C$
d	Width of the fracture, m
g	Acceleration of gravity, $m/sec^2$
h	Well depth, m
$h_p$	Heat transfer coefficient of the drill pipe, $kJ/sec-m^2-^{\circ}C$
k	Thermal conductivity of the rock, $kJ/sec-m-^{\circ}C$
q	Flow rate of the fluid, $kg/sec$
r	Drill bit size, m
$r_p$	Drill stem OD, m
s	Specific heat of the fluid, $kJ/kg-^{\circ}C$
$t_o$	Time period of drilling, sec
$A_i$	$A_i = H_i / sq$ , $1/m$
$H_i$	Heat transfer coefficients, $i=1,2$ , $kJ/sec-m-^{\circ}C$
$K_p$	Permeability of the rock, $m^2$
Q	Heat accumulation per unit time, $kJ/sec$
$T_a$	Temperature of the fluid in the annulus, $^{\circ}C$
$T_f$	Temperature of the rock formation, $^{\circ}C$
$T_i$	Inlet temperature of the fluid injection into the fracture, $^{\circ}C$
$T_o$	Initial temperature of the fluid as the drilling ceases, $^{\circ}C$
$T_p$	Temperature of the fluid in the drill pipe, $^{\circ}C$

LIST OF SYMBOLS AND UNITS (Concluded)

- $T_{pi}$  Inlet temperature of the drilling fluid, °C
- $T_s$  Surface earth temperature, °C
- $T_{AO}$  Outlet temperature at the top of the annulus, °C
- $T_{BHT}$  Bottom-Hole temperature, °C
- $U$  Heat transfer coefficient of the annulus,  $\text{kJ}/\text{sec}\cdot\text{m}^2\cdot^\circ\text{C}$
- $\alpha$  Geothermal gradient, °C/m
- $\alpha_o$  Coefficient of thermal expansion,  $1/^\circ\text{C}$
- $\rho$  Density of the rock,  $\text{kg}/\text{m}^3$
- $\rho_w$  Density of the fluid,  $\text{kg}/\text{m}^3$
- $\nu$  Viscosity of the fluid,  $\text{m}^2/\text{sec}$

## LIST OF TABLES

Table		Page
1.	Parameters in Some Typical Drilling Systems . .	9
2.	A Comparison Between Holmes and Swift 1970 Model and the Approximation Value of $T_{AO}$ and $T_{BHT}$ . . . . .	14
3.	Typical Well Data for a Geothermal Borehole . .	20
4.	Well and Fluid Properties for a Borehole- Fracture System . . . . .	35

## LIST OF ILLUSTRATIONS

Figure		Page
1.	Schematic of Circulating Borehole System. . . . .	5
2.	Temperature Profile for a Simulated Borehole. . . . .	11
3.	Temperature Data from a Borehole (G-3) in the Reykjavik Geothermal Area in Iceland. . . . .	16
4.	Temperature Field with Non-Linear Geothermal Gradient . . . . .	17
5.	Temperature Profiles for a Simulated Borehole with Non-Linear Geothermal Gradient in the Formation . . . . .	22
6.	Differences of the Outlet Temperature Vs. Depth with Geothermal Gradient Change at 160 m. . . . .	23
7.	Geothermal Borehole System with Fluid Loss. . . . .	25
8.	Temperature Profiles for a Simulated Borehole with 10% Fluid Loss. . . . .	29
9.	Temperature Profiles for a Simulated Borehole with a Fracture Located Halfway from the Surface . . . . .	30
10.	Borehole-Fracture System with a Horizontal Fracture. . . . .	32
11.	Temperature Distribution in the Fracture after One Month . . . . .	37
12.	Temperature Distribution in the Fracture at 100 Meters away from the Borehole. . . . .	38
13.	Temperature Disturbance in the Vicinity of a Fracture . . . . .	39
14.	Temperature Vs. Relaxation Time . . . . .	43
15.	Temperature Data from a Borehole (MG-16) in the Reykir Geothermal Area in Iceland . . . . .	44



## SUMMARY

Quick, reliable borehole temperature data is the most important information to be obtained in geothermal drilling. Unfortunately, the drilling process itself disturbs the surrounding temperature field. This is especially true when the temperature field is disturbed by flow of drilling fluid in fractured rocks, which is very likely in the geothermal areas.

Starting with the model by Jaeger (1961) and Holmes and Swift (1970), modified models are constructed to simulate borehole temperatures in the case of (1) non-uniform thermal conductivity in the formation and (2) loss of drilling fluid into fractures intersected by a borehole. Comparison of the calculated relaxation time for the drilling disturbance in the case of fluid loss, with the relaxation time indicated by the available data, suggests that the temperature perturbation associated with influx of the drilling fluid into a zone of fractured rocks is removed by convective processes. The effective permeability of such a fracture zone may be of the order of  $4 \times 10^{-11} \text{ m}^2$ .

## CHAPTER I

### INTRODUCTION AND RELATED WORK

The temperature field is one of the main physical characteristics of geothermal systems. Temperature observations in boreholes therefore provide some of the most important field data both in regional reconnaissance exploration for geothermal resources and in the investigation of individual reservoirs. Moreover, the temperature can be observed with a greater precision than almost any other field quantity. At temperatures below 200°C, a precision of  $10^{-2}^{\circ}\text{C}$  can be easily obtained with the help of thermister devices. Other types of thermometers are preferred at higher temperatures, for example, vapor pressure and thermoelastic devices which are less precise than the thermisters.

The drilling process itself disturbs the subsurface temperature field (1) by conductive cooling of the rock and (2) by invasion of the drilling fluid into permeable formations. Because the thermal conductivity of rock is small, such drilling disturbances have a long relaxation time. The long relaxation time becomes a problem of practical concern when decisions have to be made regarding deepening or abandoning a borehole. To avoid costly delay at the drill site, non-equilibrium temperature data are often obtained and attempts are made to extrapolate these data to obtain

estimates of the equilibrium values. The temperature of the drilling fluid at the well-head is also monitored, since it furnishes some information on formation temperature at depth. Monitoring fluid level in the mud pit indicates fluid gains or losses.

Little theoretical literature exists on borehole temperatures, particularly with regard to the complexities encountered in active geothermal areas. Bullard (1947) and Lachenbruch and Brewer (1959) have estimated the relaxation time for a borehole after it had been completed on the basis of a simple heat conduction model. Their results show that the true equilibrium is reached only after times of the order of months or years. Also only a few papers have been written on the disturbances due to drilling, taking into account the circulation of drilling fluid in the borehole. Jaeger (1961) and Holmes and Swift (1970) have given steady-state approximations to temperatures in the drilling fluid during drilling. Time-dependent calculations have been carried out by Raymond (1969) and Keller, et al. (1973). However, all of the above models have assumed both simple formation temperatures and no gains or losses of drilling fluid. No attention has been paid to the problem of interpretation of the outlet temperature.

Recently, Bodvarsson (1973) has discussed examples of temperature inversions which have been observed in geothermal areas. He suggests that such temperature inversions may

result from drilling disturbances. There have apparently been no investigations of the relaxations of temperature inversions due to drilling disturbances.

The object of this study was to investigate the information which can be obtained from the temperature data by mathematical modeling of thermal processes in the drilling fluid-bore system. The theoretical results will be compared with available field data.

In Chapter II, the model of Jaeger (1961) and Holmes and Swift (1970) will be reviewed. This will serve as the basic model. For convenience, the notations, equations and figures used by Holmes and Swift (1970) will be retained with only a slight change. An approximation method of estimating the outlet temperature and the bottom-hole temperature will be introduced. Two further modifications to the basic model, the non-linear gradient model and the fluid-loss model, will also be included in this chapter.

Chapter III will treat mainly the problem of relaxation of the drilling disturbance created by fluid losses. Temperature distributions of fluids that are lost into a fracture will be described. Temperature disturbances resulting from the drilling fluid loss and the relaxation after the drilling ceases will be investigated. The application of the fluid-loss model will also be discussed.

## CHAPTER II

### MODELING OF THE CIRCULATING BOREHOLE SYSTEM

#### Description of the Basic Model

The circulating borehole model by Jaeger (1961) and Holmes and Swift (1970) is basically a counterflow heat exchanger (Figure 1). The drilling fluid is injected at a constant temperature  $T_{pi}$  and constant flow rate  $q$ . The fluid flows down the drill pipe to the bottom ( $z = h$ ) and circulates up the surrounding annulus. Heat is transported by convection within the borehole and by conduction in the rock formation.

#### The Basic Equations

Several assumptions are made to obtain the basic equations:

(1) Axial conduction of heat in the fluid is negligible compared with axial convection.

(2) There is no radial gradient in the fluid in either the drill pipe or the annulus.

(3) The fluid's properties (heat capacity, density, and thermal conductivity) do not change significantly with temperature.

(4) Heat generation by viscous dissipation in the fluid is negligible.

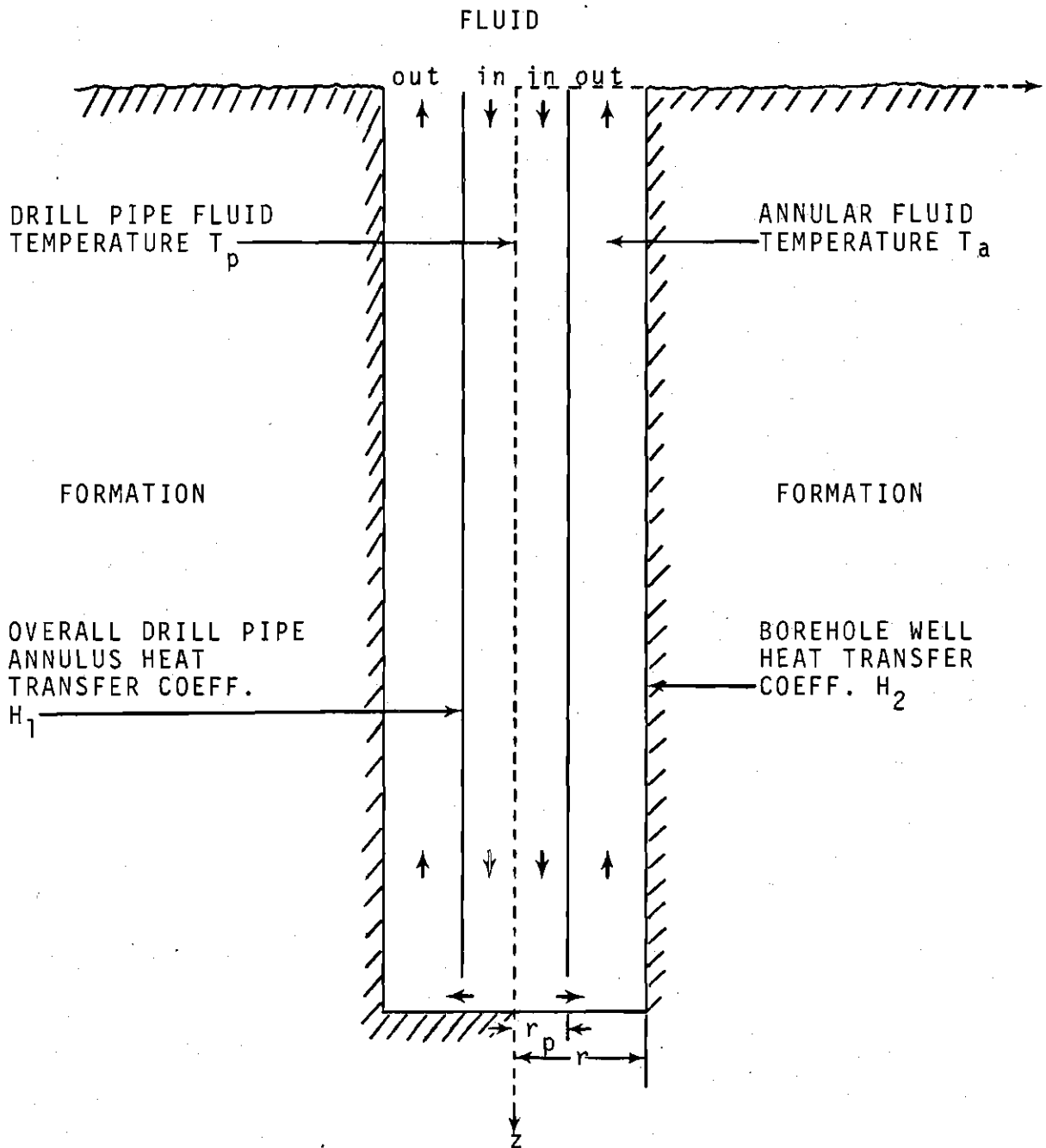


Figure 1. Schematic of Circulating Borehole System.

Based on the above assumptions, the heat accumulations per unit time  $Q$  of the fluid between depth  $z$  and  $z+dz$  are given by:

$$Q_p(z) - Q_p(z+dz) = sq(T_p(z) - T_p(z+dz))$$

$$Q_a(z) - Q_a(z+dz) = sq(T_a(z) - T_a(z+dz))$$

where the subscripts  $a$  and  $p$  indicate the quantities in the annulus and the drill pipe respectively,  $s$  is the specific heat of the fluid, and  $q$  is the flow rate of the drilling fluid.

The heat transfer between the drill pipe and the annulus  $Q_{ap}$  is given by:

$$Q_{ap}(z) = H_1(T_p(z) - T_a(z))dz$$

Similarly the heat transfer between the annulus and the rock formation  $Q_{fa}$

$$Q_{fa}(z) = H_2(T_a(z) - T_f(z))dz$$

where  $f$  indicates the quantities in the formation,  $H_1$  and  $H_2$  are the heat transfer coefficients across the drill pipe and the wellbore face, respectively.

Combining these equations gives the overall heat

balance through the pipe and annulus:

$$sq \frac{dT_p(z)}{dz} = H_1 (T_a(z) - T_p(z)) \quad (1)$$

$$sq \frac{dT_a(z)}{dz} = H_1 (T_a(z) - T_p(z)) + H_2 (T_a(z) - T_f(z))$$

With a linear geothermal gradient  $\alpha$  and a given surface earth temperature  $T_s$ , formation temperature  $T_f$  can be represented by a linear relation

$$T_f(z) = T_s + \alpha z \quad (2)$$

To solve equations (1), (2), two boundary conditions are needed:

(1) Inlet temperature  $T_{pi}$  is a constant:

$$T_p(0) = T_{pi}$$

(2) The drilling fluids are mixed at the bottom:

$$T_p(h) = T_a(h)$$

The solution will be

$$T_p(z) = K_1 \exp(C_1 z) + K_2 \exp(C_2 z) + T_s + \alpha z - \alpha/A_1 \quad (3)$$



$$T_a(z) = K_1(1 + C_1/A_1) \exp(C_2 z) + K_2(1 + C_2/A_1) \exp(C_2 z) + T_s + \alpha z \quad (3)$$

where

$$A_1 = H_1 / sq \quad (4)$$

$$A_2 = H_2 / sq$$

$$C_1 = (A_2/2) (1 + (1 + 4A_1/A_2)^{1/2}) \quad (5)$$

$$C_2 = (A_2/2) (1 - (1 + 4A_1/A_2)^{1/2})$$

$$K_1 = -((T_{pi} - T_s + \alpha/A_1) C_2 \exp(C_2 h) + \alpha) / (C_1 \exp(C_1 h) - C_2 \exp(C_2 h)) \quad (6)$$

$$K_2 = ((T_{pi} - T_s + \alpha/A_1) C_1 \exp(C_1 h) + \alpha) / (C_1 \exp(C_1 h) - C_2 \exp(C_2 h))$$

The well data used to construct temperature profiles are given in Table 1.

The heat transfer coefficients given in Table 1 have taken account of the wellbore size and computed according to the relations:

$$H_1 = 2\pi r_p h_p$$

$$H_2 = 2\pi r U$$

Table 1. Parameters in Some Typical Drilling Systems\*

model	$H_1$	$H_2$	s	q	$T_{pi}$	$T_s$	$\alpha$	h
1	.09	.003	4	15	30	20	.025	5000
2	.15	.003	4	15	30	20	.025	5000
3	.03	.003	4	15	30	20	.025	5000
4	.09	.0045	4	15	30	20	.025	5000
5	.09	.0015	4	15	30	20	.025	5000
6	.09	.003	4	10	30	20	.025	5000
7	.09	.003	4	20	30	20	.025	5000

\*Converted to MKS units from the data of Holmes and Swift (1970)

Where  $r_p$ ,  $r$  are the radius of the drill pipe and the well-bore.  $U$  and  $h_p$  represent the heat transfer coefficients used by Holmes and Swift (1970). They assumed that the radius of the drill pipe was  $r_p = 16.84$  cm. and of the annulus was  $r_a = 21.27$  cm.

For example, the temperature profiles of the drilling fluid in the pipe and the annulus of model 1 are shown in Figure 2. The annulus temperature is greater than the pipe temperature at every depth in the borehole due to the additional heat transfer from the rock formation. The drilling fluid becomes heated up in the upper half of the borehole and cooled down in the lower half. Holmes and Swift (1970) have shown that the steady-state model is useful for predicting bottom-hole temperatures.

As can be seen from Table 1, the seven models differ as a result of different heat transfer coefficients or mud circulation rate. The differences in parameters will cause the temperature profiles to be slightly different, although of the same basic shape as in Figure 1. The outlet temperature and bottom-hole temperature for the various models in Table 1 will be used for comparison with further approximations which will be made in the next section.

#### Further Approximation to the Outlet Temperature and the Bottom-Hole Temperature

The temperature  $T_{AO}$ , is the temperature of the drilling

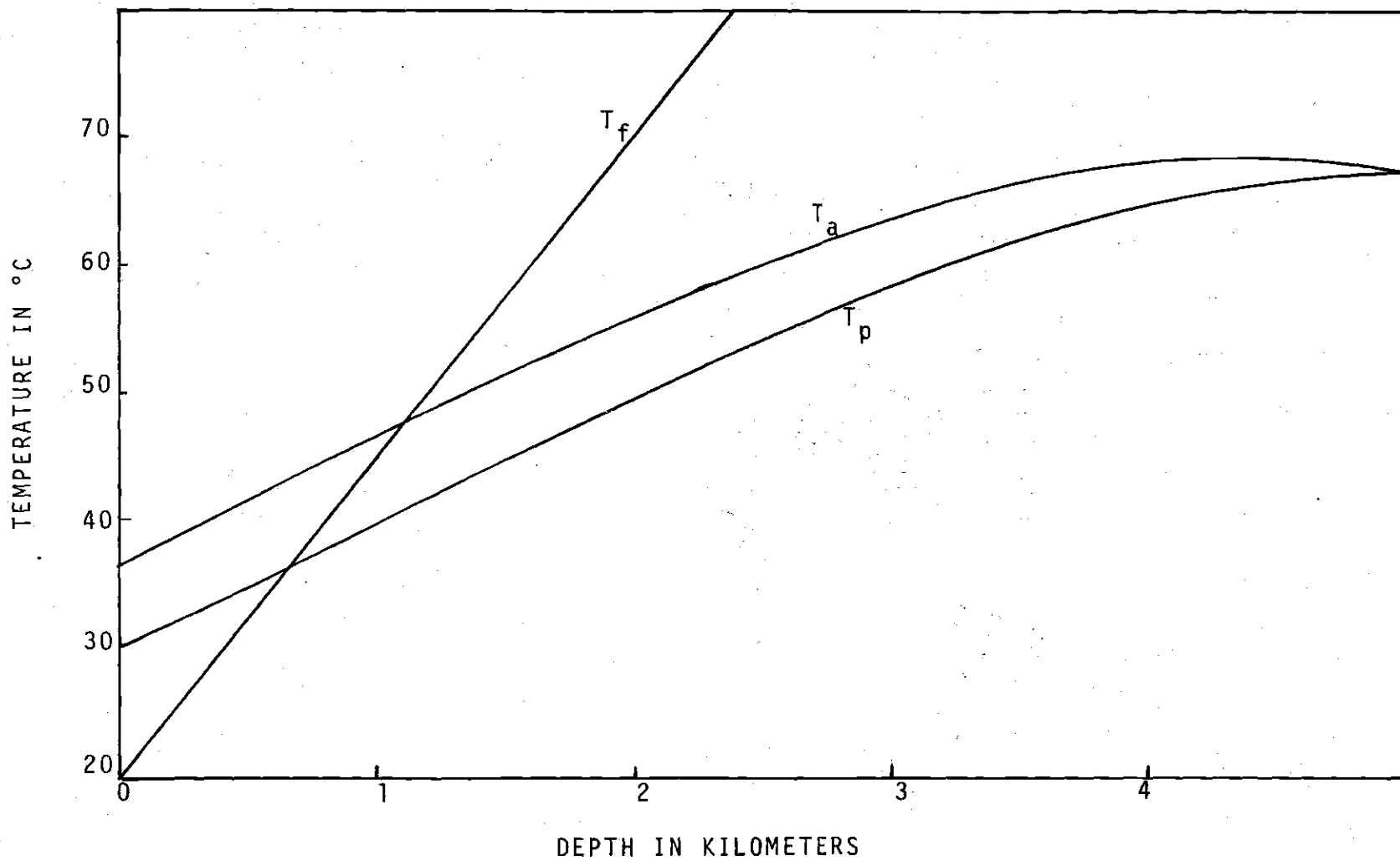


Figure 2. Temperature Profiles for a Simulated Borehole.

fluid exiting the borehole (the outlet temperature). Data on the outlet temperature is fairly easily obtained and furthermore, it can be measured even as the drilling is in progress. The measurements of the outlet temperature can yield useful information regarding the down-hole situation; however, because of complicated heat transfer processes in the borehole, this information may be difficult to extract. On the other hand, the bottom-hole temperature  $T_{BHT}$ , although more difficult to measure, tends to reach equilibrium the quickest after drilling ceases (Bullard, 1947). Hence  $T_{BHT}$  is often a useful indicator of the down-hole situations.

$T_{AO}$  and  $T_{BHT}$  can be calculated from equations (3).

$$T_{AO} = T_a(0) = K_1(1 + C_1/A_1) + K_2(1 + C_2/A_1) + T_s \quad (7)$$

$$T_{BHT} = T_a(h) = T_p(h) = K_1 \exp(C_1 h) + K_2 \exp(C_2 h) + T_s + \alpha h - \alpha/A_1$$

Since, in general, the heat transfer coefficient across the drilling pipe is much greater than across the wellbore face, further approximations can be made.

Assuming

$$H_1 \gg H_2$$

$$A_1/A_2 = H_1/H_2 \gg 1.$$

Then  $C_1$  can be approximated by

$$C_1 = (A_2/2)(1 + (1 + 4A_1/A_2)^{1/2})$$

$$\doteq (A_2/2)(1 + 2(A_1/A_2)^{1/2})$$

$$\doteq (A_1 A_2)^{1/2}$$

Similarly

$$C_2 \doteq -(A_1 A_2)^{1/2}$$

Substitute  $C_1, C_2$  into equations (6).

$$K_1 = \frac{1}{2}((T_{pi} - T_s + \alpha/A_1) \exp(-(A_1 A_2)^{1/2} h) - \alpha/(A_1 A_2)^{1/2}) \operatorname{sech}((A_1 A_2)^{1/2} h)$$

$$K_2 = \frac{1}{2}((T_{pi} - T_s + \alpha/A_1) \exp(+ (A_1 A_2)^{1/2} h) + \alpha/(A_1 A_2)^{1/2}) \operatorname{sech}((A_1 A_2)^{1/2} h)$$

Substitute  $C_1, C_2, K_1, K_2$  into equations (7).

$$T_{BHT} = (T_{pi} - T_s + \alpha/A_1) \operatorname{sech}((A_1 A_2)^{1/2} h) - (\alpha/(A_1 A_2)^{1/2}) \tanh((A_1 A_2)^{1/2} h) + T_s + \alpha h - \alpha/A_1 \quad (8)$$

$$T_{AO} = (T_{pi} - T_s + \alpha/A_1)(1 - A_2/A_1)^{1/2} \tanh((A_1 A_2)^{1/2} h) + T_s - (\alpha/A_1) \operatorname{sech}((A_1 A_2)^{1/2} h) \quad (9)$$

Instead of equations (3), equations (8), (9) provide means for quick estimation of  $T_{AO}$  and  $T_{BHT}$  without computing the constants  $C_1$ ,  $C_2$ ,  $K_1$ ,  $K_2$ . Table 2 gives the values calculated from equations (3), the approximated values from (8) and (9) and ratios of the heat transfer coefficients for each model in Table 1.

Table 2. A Comparison Between the Holmes and Swift (1970) Model and Approximated Values of  $T_{AO}$  and  $T_{BHT}$ .

Model	$T_{BHT}$			$T_{AO}$		
	H. & S. (1970)	Approx.	$H_1/H_2$	H. & S. (1970)	Approx.	$H_1/H_2$
1	67.571	60.873	30	36.244	34.428	30
2	79.602	74.929	50	34.770	34.014	50
3	47.056	35.988	10	38.838	29.883	10
4	76.088	69.503	20	37.175	35.086	20
5	54.249	49.476	60	34.313	33.029	60
6	85.814	80.326	30	35.577	34.578	30
7	56.001	49.182	30	36.024	33.570	30

As shown in Table 2, provided  $H_1/H_2 > 20$ , the approximated values are quite close to, although less than, the acceptable values given by Holmes and Swift. As a result, the approximated values represent the lower limit of both

$T_{BHT}$  and  $T_{AO}$ . Moreover for high ratios of  $H_1/H_2$ , the simple relations (8) and (9) provide a quick way to determine geothermal gradients. With measured values of  $T_{AO}$  and  $T_{BHT}$ ,  $\alpha$  can be estimated to satisfy both equations.

### The Model with Non-Linear Geothermal Gradients

In the basic model, a constant geothermal gradient is used. However, the temperature measurements in boreholes in the major geothermal regions have shown that the reservoir temperature is rather uniform below a certain depth. This situation is indicative of a high permeability, since convective flows in the reservoir tend to equalize the temperature in the rock. The reservoir temperature within the uniform part of the formation is called the base temperature of the thermal area; and since this is the region from which thermal water is produced, it is useful to know the depth to this part of the formation. Figure 3 shows the temperature data from a borehole (G-3) in the Reykjavik thermal area in Iceland. Temperature increases quite rapidly in the upper 160 meters and then becomes practically constant beyond this depth. The base temperature is around 130°C.

A slight modification of the basic model can be used to simulate this situation. Instead of the constant geothermal gradient  $\alpha$ , a zero gradient is replaced for the lower section of the rock formation as in Figure 4.



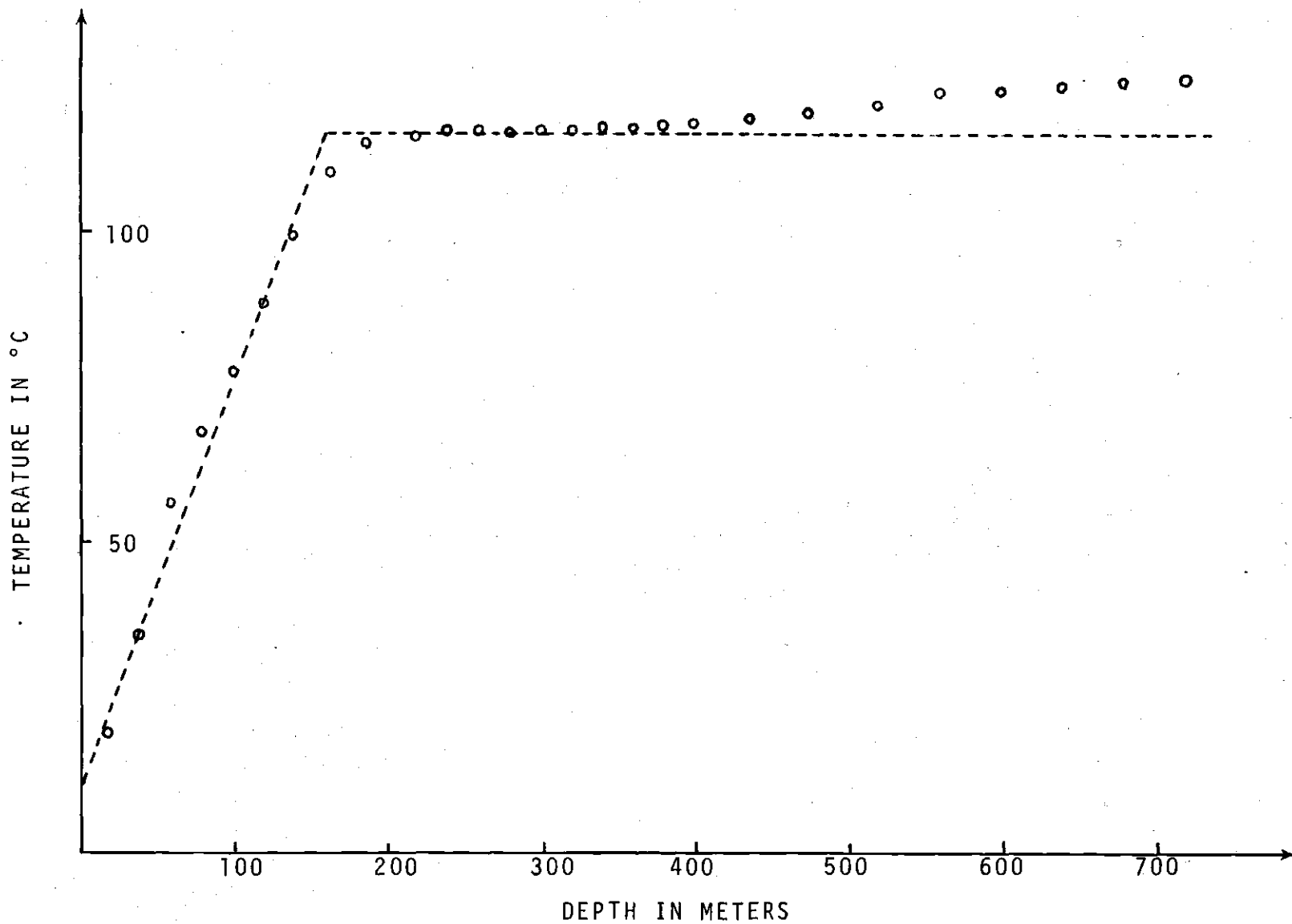


Figure 3. Temperature Data from a Borehole (G-3) in the Geothermal Area in Iceland (Reproduced from Sigurmundsson 1967). Broken Line is the Non-Linear Model Used.

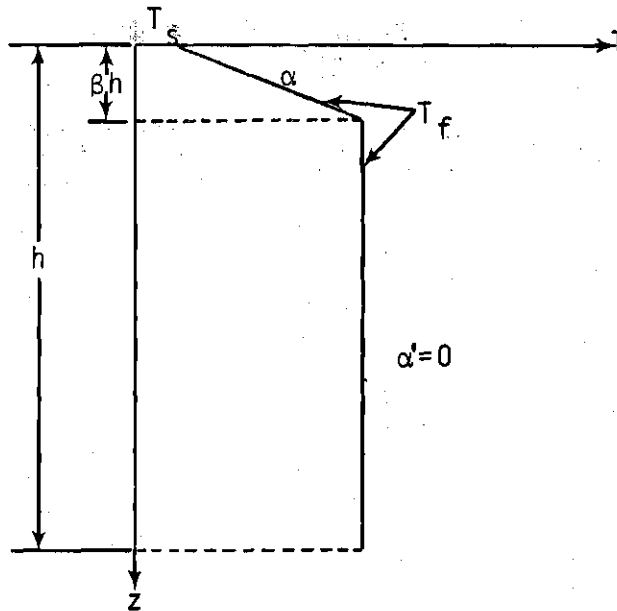


Figure 4. Temperature Field with Non-Linear Geothermal Gradient.

Thus the formation temperature can be represented by

$$T_f(z) = T_s + \alpha z \quad 0 \leq z \leq \beta h \quad (10a)$$

$$T_f(z) = T_s + \alpha \beta h \quad \beta h \leq z \leq h \quad (10b)$$

The solution in the upper section  $0 \leq z \leq \beta h$

$$T_p(z) = K_1 \exp(C_1 z) + K_2 \exp(C_2 z) + \alpha z - \alpha/A_1 + T_s \quad (11a)$$

$$T_a(z) = K_1 (1 + C_1/A_1) \exp(C_1 z) + K_2 (1 + C_2/A_1) \exp(C_2 z) + \alpha z + T_s$$

and in the lower section  $\beta h \leq z \leq h$

$$T'_p(z) = K'_1 \exp(C_1 z) + K'_2 \exp(C_2 z) + \alpha \beta h + T_s \quad (11b)$$

$$T'_a(z) = K'_1 (1 + C_1/A_1) \exp(C_1 z) + K'_2 (1 + C_2/A_1) \exp(C_2 z) + \alpha \beta h + T_s$$

To solve the integration constants  $K_1$ ,  $K_2$ ,  $K'_1$ ,  $K'_2$ , four boundary conditions are needed.

(1). Inlet temperature  $T_{pi}$  is a constant:

$$T_p(0) = T_{pi}$$

(2). Temperature in the drill pipe is mathematically continuous through  $z = \beta h$ :

$$T_p(\beta h) = T'_p(\beta h)$$

(3). Temperature in the annulus is mathematically continuous through  $z = \beta h$ :

$$T_a(\beta h) = T'_a(\beta h)$$

(4). The drilling fluid of the drill pipe and the annulus are well mixed at the bottom:

$$T'_p(h) = T'_a(h)$$

The computed integration constants are

$$K_1 = -((T_{pi} - T_s + \alpha/A_1)C_2 \exp(C_2 h)) \quad (12a)$$

$$\begin{aligned} & -(\alpha/A_1(C_1 - C_2))((A_1 + C_1)C_2 \exp(C_2(1-\beta)h) \\ & - (A_1 + C_2)C_1 \exp(C_1(1-\beta)h)) / (C_1 \exp(C_1 h) - C_2 \exp(C_2 h)) \end{aligned}$$

$$K_2 = ((T_{pi} - T_s + \alpha/A_1)C_1 \exp(C_1 h)) \quad (12b)$$

$$\begin{aligned} & -(\alpha/A_1(C_1 - C_2))((A_1 + C_1)C_2 \exp(C_2(1-\beta)h) \\ & - (A_1 + C_2)C_1 \exp(C_1(1-\beta)h)) / (C_1 \exp(C_1 h) - C_2 \exp(C_2 h)) \end{aligned}$$

$$K'_1 = -((T_{pi} - T_s + \alpha/A_1)C_2 \exp(C_2 h)) \quad (12c)$$

$$\begin{aligned} & -(\alpha/A_1(C_1 - C_2))((A_1 + C_1) \exp(-C_2 \beta h) \\ & - (A_1 + C_2) \exp(-C_1 \beta h)) C_2 \exp(C_2 h) / (C_1 \exp(C_1 h) - C_2 \exp(C_2 h)) \end{aligned}$$

$$K'_2 = ((T_{pi} - T_s + \alpha/A_1)C_1 \exp(C_1 h)) \quad (12d)$$

$$\begin{aligned} & -(\alpha/A_1(C_1 - C_2))((A_1 + C_1) \exp(-C_2 \beta h) \\ & - (A_1 + C_2) \exp(-C_1 \beta h)) C_1 \exp(C_1 h) / (C_1 \exp(C_1 h) - C_2 \exp(C_2 h)) \end{aligned}$$

Typical geothermal well data used to construct the temperature profile of G-3 are given in Table 3.

Table 3. Typical Well Data for a Geothermal Borehole

---

$h$	Well depth, m	720
$s$	Fluid specific heat, $\text{kJ/kg-}^\circ\text{C}$	4
$q$	Flow rate, $\text{kg/sec}$	25
$H_1$	Heat transfer coefficient (pipe), $\text{kJ/m-sec-}^\circ\text{C}$	.09
$H_2$	Heat transfer coefficient (annulus), $\text{kJ/m-sec-}^\circ\text{C}$	.003
$T_s$	Surface earth temperature, $^\circ\text{C}$	10
$T_{pi}$	Inlet temperature, $^\circ\text{C}$	10
$\alpha$	Geothermal gradient for the upper section, $^\circ\text{C/m}$	.675
$\alpha'$	Geothermal gradient for the lower section, $^\circ\text{C/m}$	0
$h$	Depth for the upper section, m	160

---

The temperature profiles shown in Figure 5 are depicted in an expanded scale of temperature. Due to the shallow depth and rather high flow rate used, the temperature in the drill pipe increases less than  $.8^{\circ}\text{C}$  at the bottom.

The calculation of the outlet temperature  $T_{AO}$  based on equation (11a) suggests that differences in  $T_{AO}$  as the drilling proceeds to greater depths may be indicative of the changing temperature gradient. Let  $T_{AO} = (T_{AO})_h - (T_{AO})_{h-10}$ , where  $(T_{AO})_h$  represents the outlet temperature when the depth of the borehole is  $h$  and  $(T_{AO})_{h-10}$  represents the outlet temperature when the depth of the borehole is 10 meters less than  $h$ . Figure 6 shows that  $T_{AO}$  increases with depth in the region where the geothermal gradient increases. However, in the uniform part of the formation  $T_{AO}$  is essentially independent of the well depth. This suggests that the careful measurements of the outlet temperatures may show where the producing part of the reservoir borehole has reached.

#### The Model with Fluid Losses

It has been suggested (Bodvarsson, 1973) that in many cases the anomalous features of field data can be explained in terms of a drilling disturbance involving drilling fluid invasion into permeable fractures. The basic model can also be modified to allow the possibility of gains and losses of the drilling fluid. Since the horizontal permeability in geothermal areas frequently is due to narrow horizontal fractures (Bodvarsson, 1970), it is expected that the drilling

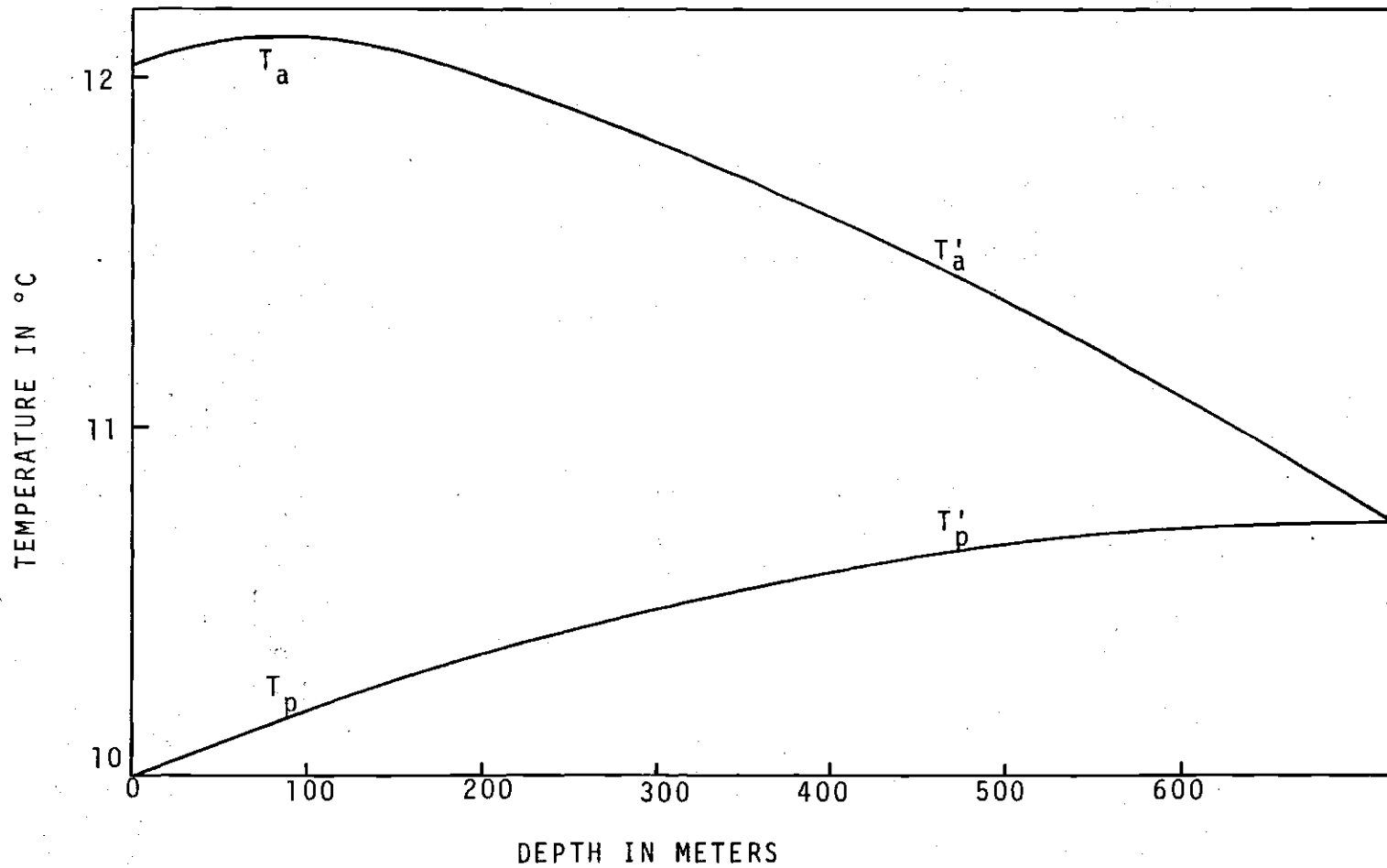


Figure 5. Temperature Profiles for a Simulated Borehole with Non-Linear Geothermal Gradient in the Formation.

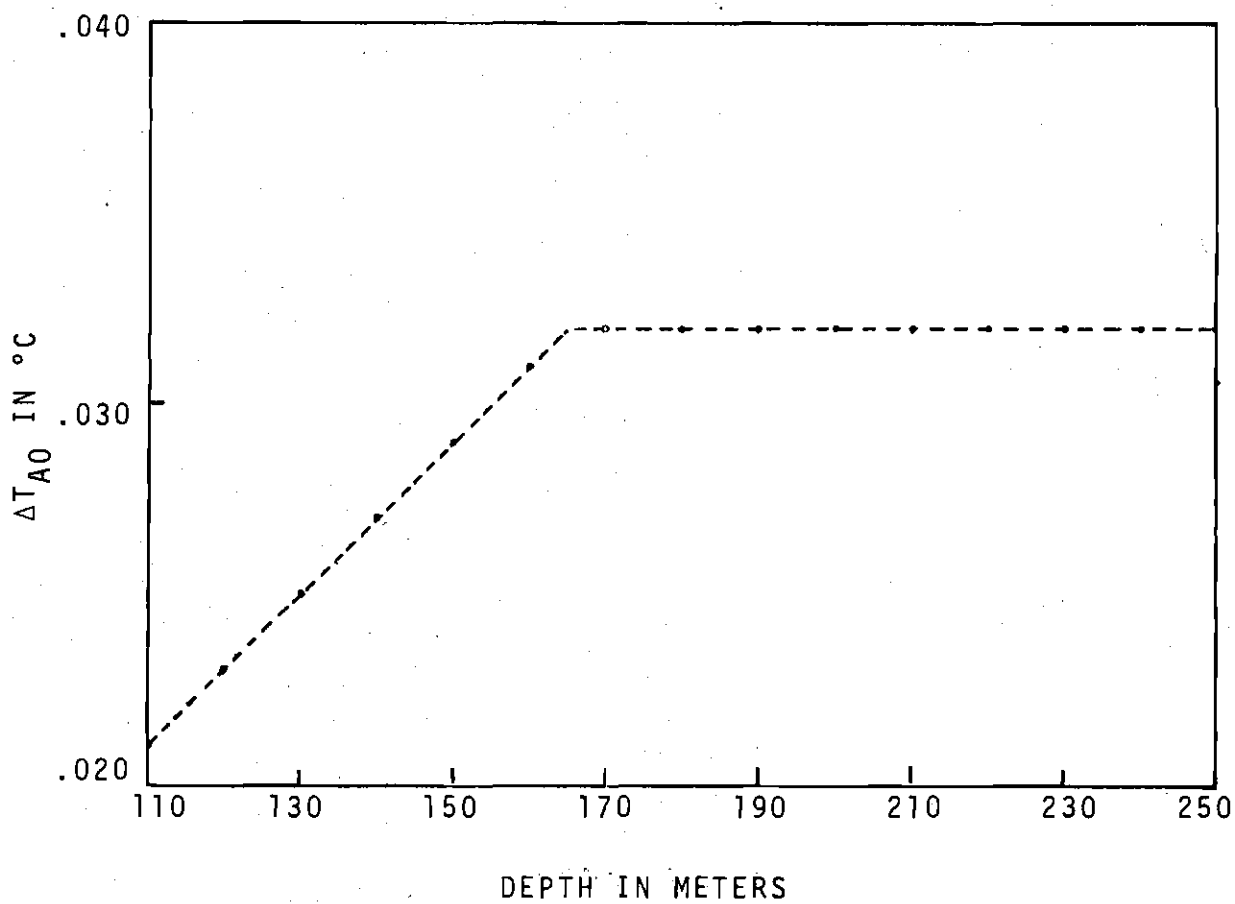


Figure 6. Differences of the Outlet Temperatures Vs. Depth with Geothermal Gradient Change at 160 m.



fluid may invade these fractures and flow away from the borehole. Similarly, the influx of geothermal fluids will also be characterized by radial flow in thin horizontal fractures.

Let  $(0 \leq \beta \leq 1)$  be the ratio of the depth of the fracture to the total depth of the borehole, then  $\beta h$  indicates the location of the fracture. Also let  $\gamma$  be the ratio of the flow rate in the annulus above the fracture to the original flow rate; the fluid losses or gains will thus be represented by  $1-\gamma$ . The modified system is depicted in Figure 7.

As in the preceding case, the borehole is divided into two sections. The basic equations for the section above the fracture are

$$\frac{dT_p(z)}{dz} + A_1(T_p(z) - T_a(z)) = 0 \quad 0 \leq z \leq \beta h \quad (13)$$

$$\gamma \frac{dT_a(z)}{dz} + A_1(T_p(z) - T_a(z)) + A_2(T_f(z) - T_a(z)) = 0$$

And for the section below the fracture

$$\frac{dT'_p(z)}{dz} + A_1(T'_p(z) - T'_a(z)) = 0 \quad \beta h \leq z \leq h \quad (14)$$

$$\frac{dT'_a(z)}{dz} + A_1(T'_p(z) - T'_a(z)) + A_2(T_f(z) - T'_a(z)) = 0$$

where

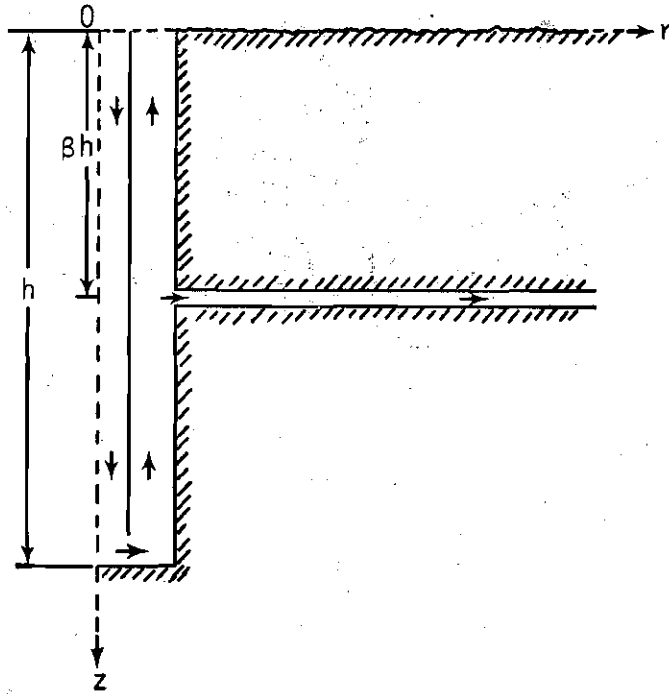


Figure 7. Geothermal Borehole System with Fluid Losses.

$$T_f(z) = T_s + \alpha z$$

The solutions to the above equations with proper boundary conditions will be

$$T_p(z) = K_1 \exp(C_1 z) + K_2 \exp(C_2 z) + \alpha(z - 1/A_1 - (1-\gamma)/A_2) + T_s \quad (15)$$

$$T_a(z) = K_1(1 + c_1/A_1) \exp(C_1 z) + K_2(1 + C_2/A_1) \exp(C_2 z) + \alpha(z - (1-\gamma)/A_2) + T_s$$

$$T'_p(z) = K'_1 \exp(C_1 z) + K'_2 \exp(C_2 z) + \alpha(z - l/A_1) + T_s$$

(16)

$$T'_a(z) = K'_1 (1 + C_1/A_1) \exp(C_1 z) + K'_2 (1 + C_2/A_1) \exp(C_2 z) + \alpha z + T_s$$

where the constants are

$$C_1 = \left( \frac{((1-\gamma)A_1 + A_2)/2\gamma}{1 + (1 + 4\gamma A_1 A_2 / ((1-\gamma)A_1 + A_2)^{1/2})^2} \right)^{1/2}$$

$$C_2 = \left( \frac{((1-\gamma)A_1 + A_2)/2\gamma}{1 - (1 + 4\gamma A_1 A_2 / ((1-\gamma)A_1 + A_2)^{1/2})^2} \right)^{1/2}$$

$$C'_1 = (A_2/2) (1 + (1 + 4A_1/A_2)^{1/2})$$

$$C'_2 = (A_2/2) (1 - (1 + 4A_1/A_2)^{1/2})$$

The boundary conditions are the same as in the preceding fracture model.

$$(1). \quad T_p(0) = T_{pi}$$

$$(2). \quad T_p(\beta h) = T'_p(\beta h)$$

$$(3). \quad T_a(\beta h) = T'_a(\beta h)$$

$$(4). \quad T'_p(h) = T'_a(h).$$

With all the above boundary conditions, constants  $K_1$ ,  $K_2$ ,  $K_1'$ ,  $K_2'$  are found to be

$$\begin{aligned}
 K_1 D = & (T_{pi} - T_s + \alpha(1/A_1 + (1-\gamma)/A_2)) (C_2'(C_2 - C_1') \exp((C_2 + C_1')\beta h)) \quad (17a) \\
 & + C_1'(C_2' - C_2) \exp((C_1' - C_2' + (C_2 + C_2')\beta)h) \\
 & - \alpha h (C_1' - C_2') \exp(((C_1' + C_2')\beta - C_2')h) \\
 & + ((1-\gamma)C_1' C_2' \alpha / A_2) (\exp(C_1' \beta h) - \exp((C_2' \beta + C_1' - C_2')h))
 \end{aligned}$$

$$\begin{aligned}
 K_2 D = & (T_{pi} - T_s + \alpha(1/A_1 + (1-\gamma)/A_2)) (C_2'(C_1' - C_1) \exp((C_1' + C_1)\beta h)) \quad (17b) \\
 & + C_1'(C_1 - C_2') \exp((C_1' - C_2' + (C_1 + C_2')\beta)h) \\
 & + \alpha h (C_1' - C_2') \exp(((C_1' + C_2')\beta - C_2')h) \\
 & - ((1-\gamma)C_1' C_2' \alpha / A_2) (\exp(C_1' \beta h) - \exp((C_2' \beta + C_1' - C_2')h))
 \end{aligned}$$

$$\begin{aligned}
 K_1' D = & (T_{pi} - T_s + \alpha(1/A_1 + (1-\gamma)/A_2)) C_2'(C_2 - C_1) \exp((C_1 + C_2)\beta h) \quad (17c) \\
 & + ((1-\gamma)\alpha C_2' / A_2) (C_1 \exp(C_1 \beta h) - C_2 \exp(C_2 \beta h)) \\
 & + \alpha h \exp(-C_2' h) ((C_2' - C_1') \exp((C_1 + C_2')\beta h) \\
 & + (C_2 - C_2') \exp((C_2 + C_2')\beta h))
 \end{aligned}$$

$$\begin{aligned}
K_2'D = & (T_{pi} - T_s + \alpha(1/A_1 + (1-\gamma)/A_2))C_1'(C_1 - C_2)\exp((C_1' - C_2' + (C_1 + C_2)\beta)h) \\
& + ((1-\gamma)\alpha C_1'/A_2)\exp((C_1' - C_2')h)(C_1\exp(C_1\beta h) - C_2\exp(C_2\beta h)) \\
& + \alpha h \exp(-C_2'h)((C_1 - C_1')\exp((C_1 + C_1')\beta h) \\
& \quad + (C_1' - C_2)\exp((C_1' + C_2)\beta h))
\end{aligned} \tag{17d}$$

Where

$$\begin{aligned}
D = & C_2'(C_1' - C_1)\exp((C_1' + C_1)\beta h) + C_2'(C_2 - C_1')\exp((C_1' + C_2)\beta h) \\
& + \exp((C_1' - C_2')h)((C_1'(C_1 - C_2')\exp((C_1 + C_2')\beta h) \\
& \quad + C_1'(C_2' - C_2)\exp((C_2' + C_2)\beta h))
\end{aligned} \tag{17e}$$

Typical temperature profiles are shown in Figures 8 and 9. Data used here are the same as in Table 3, except that a deeper borehole (2000 meters) and a linear gradient (.1 °C/m) are assumed. Figure 8 shows that the temperature profile is not a sensitive function of the location of the fracture. A fluid loss of 10 percent was assumed in Figure 8. However, Figure 9 does show an obvious change related to different ratio of fluid loss.

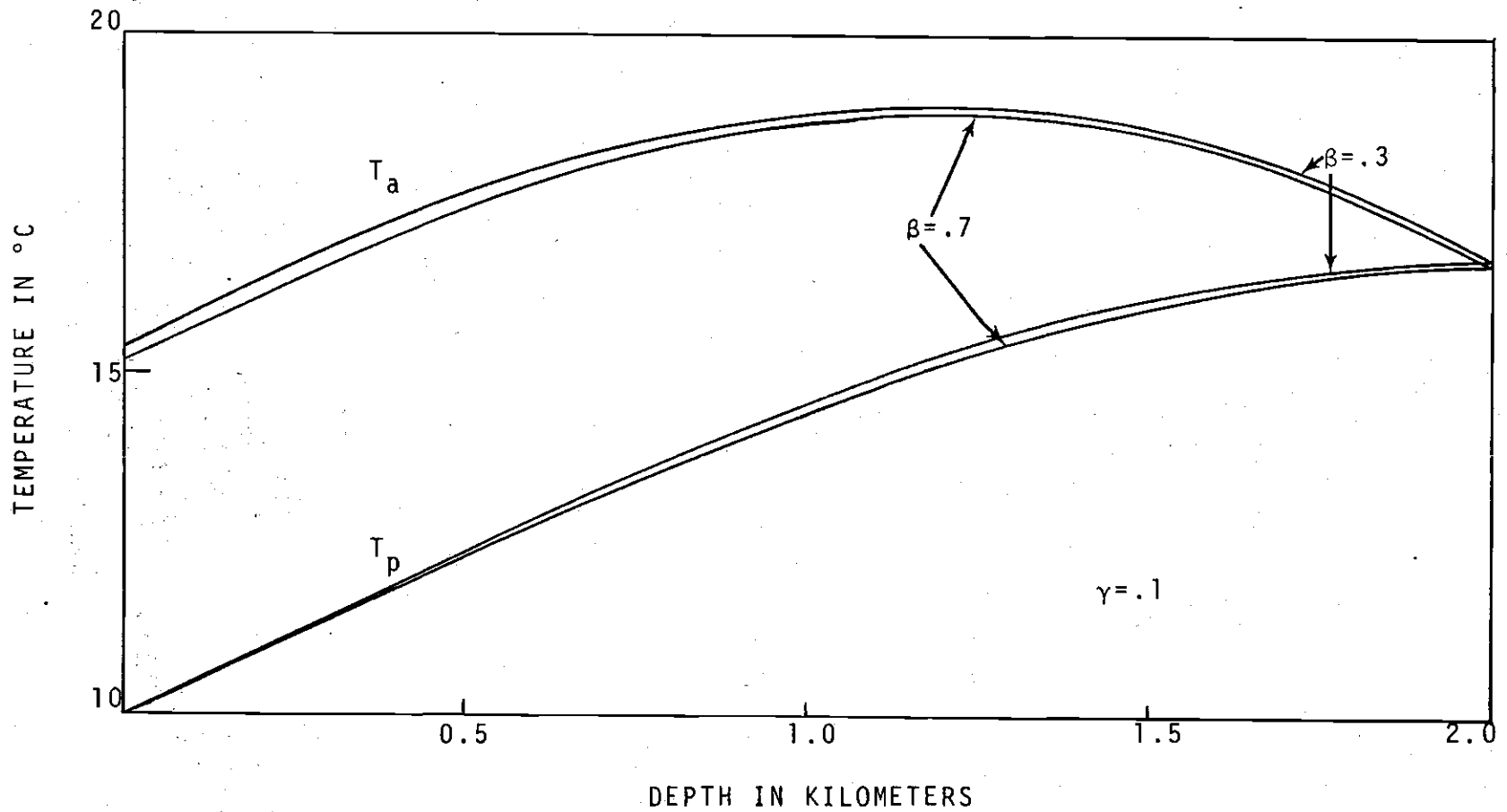


Figure 8. Temperature Profiles for a Simulated Borehole with 10% Fluid Loss.  $\beta$  Indicates the Ratio of Location of the Fracture from the Top of the Borehole to the Total Depth of the Borehole.

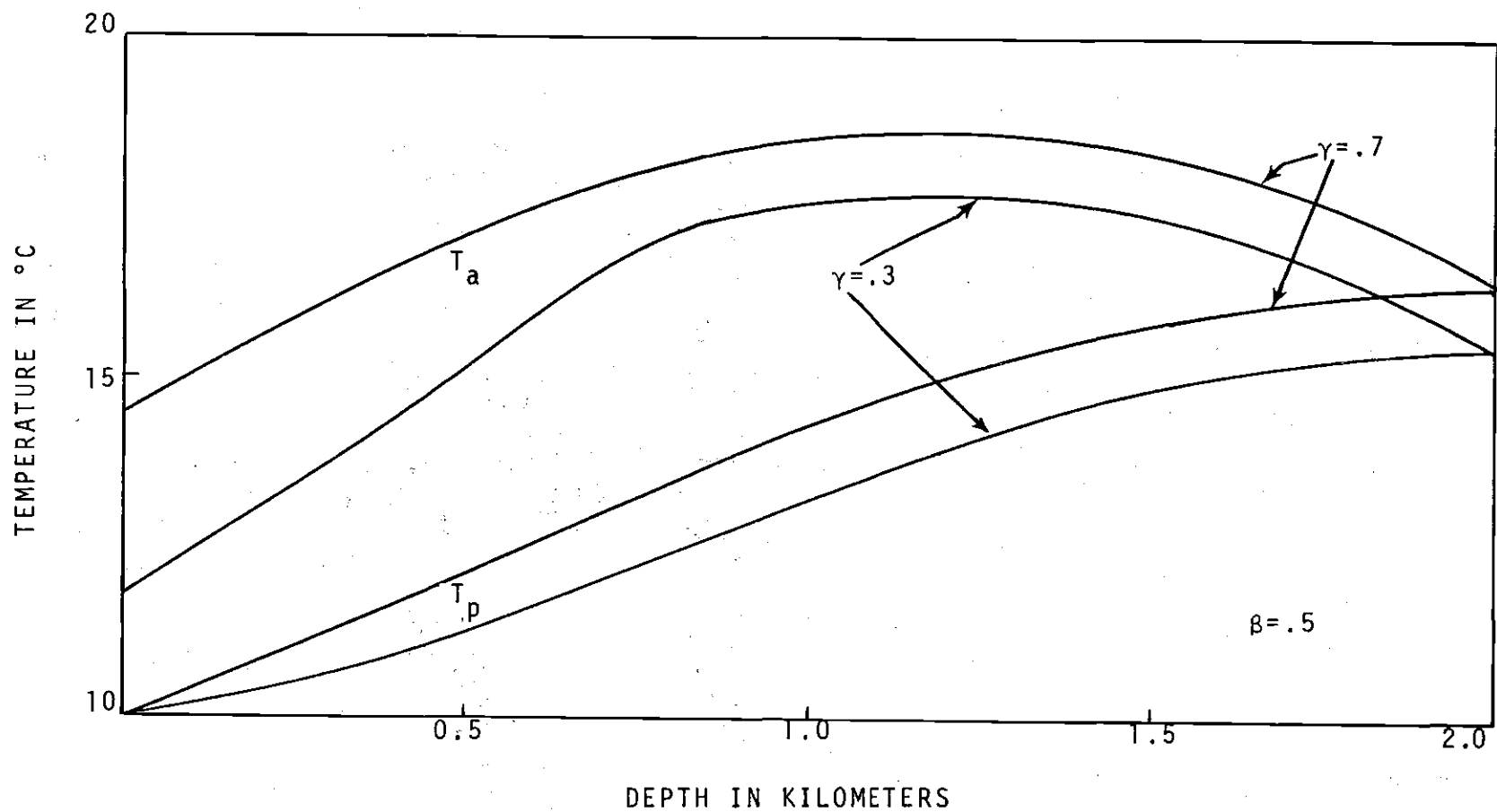


Figure 9. Temperature Profiles for a Simulated Borehole with a Fracture Located Halfway from the Surface.  $\gamma$  Indicates the Ratio of the Flow Rate above the Fracture in the Annulus to the Original Flow Rate.

## CHAPTER III

## RELAXATION OF DRILLING DISTURBANCE

Temperature Distribution of the Fluid in a Fracture

In the preceding chapter, temperature profiles for the fluid-loss model are obtained; however, the effect of invasion of the drilling fluid into permeable formations have not been considered. Assume the drilling fluid is injected into a relatively hotter formation. The cooling effect will disturb the surrounding temperature field and eventually change the temperature profiles. Bodvarsson (1973) derived theoretical models for the temperature behavior of a fluid injected into a fracture. These models will be derived below and used to describe the temperature perturbation due to the loss of drilling fluid into a fracture.

Assuming the drilling fluid invades into a sheet-like horizontal fracture with an initial temperature  $T_i$  at time  $t=0$ . The formation temperature is a constant  $T_f$  (Figure 10).

The heat transport problem now consists of pure conduction between the fracture and the rock formation and pure convection along the fracture. Let  $a$  be the thermal diffusivity of the rock. The temperature of the rock is determined from the heat equation.



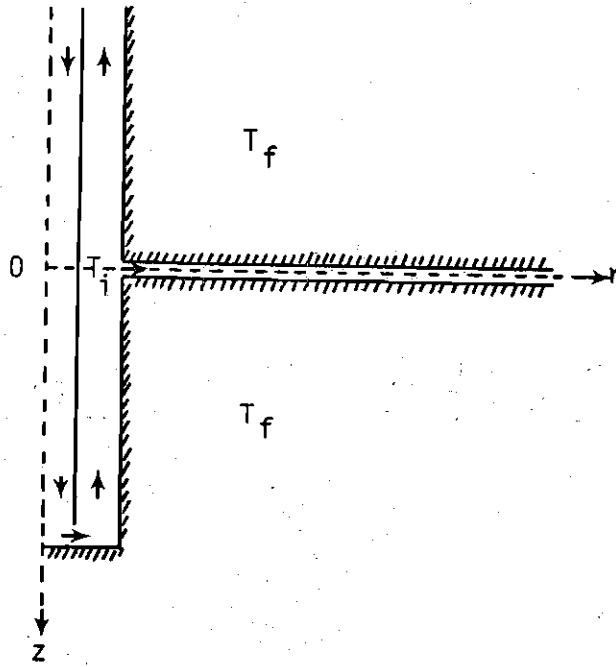


Figure 10. Geothermal Borehole System with a Horizontal Fracture.

$$\frac{\partial^2 T}{\partial r^2} + \frac{1}{r} \frac{\partial T}{\partial r} + \frac{\partial^2 T}{\partial z^2} = \frac{1}{\alpha} \frac{\partial T}{\partial t} \quad (18)$$

The convective transport appears in the boundary condition at the wall of the fracture.

Heat transport by the fluid = Heat conducted through  
the rock surface

$$\rho_w s d \frac{dT}{dt} = \rho_w s d \frac{\partial T}{\partial t} + s q \frac{\partial T}{\partial r} = 4\pi r k \frac{\partial T}{\partial z} \quad \text{at } z=0 \quad (19)$$

Where  $\rho_w$  = density of the fluid

$s$  = specific heat of the fluid

$d$  = width of the fracture (vertical)

$q$  = flow rate of the fluid

$k$  = thermal conductivity of the rock

Two further approximations will be made in order to solve the conduction equation (Bodvarsson, 1969). First, neglect conduction in the radial direction.

$$\frac{1}{r} \frac{\partial}{\partial r} \left( r \frac{\partial T}{\partial r} \right) \ll \frac{\partial^2 T}{\partial z^2}$$

Also, the vertical width of the fracture is assumed to be so small that

$$\left| \rho_w s d \frac{\partial T}{\partial t} \right| \ll \left| s q \frac{\partial T}{\partial r} \right|$$

The transport equations (18), (19) then reduce to

$$\frac{\partial^2 T}{\partial z^2} = \frac{1}{a} \frac{\partial T}{\partial t} \quad (20)$$

$$\frac{\partial T}{\partial r} = \frac{4\pi rk}{sq} \frac{\partial T}{\partial z}, \quad z=0 \quad (21)$$

Make the substitutions  $b = \frac{2k}{sq}$ ,  $A = \pi r^2$ , equations (20), (21) become

$$\frac{\partial^2 T}{\partial z^2} = \frac{1}{a} \frac{\partial T}{\partial t} \quad (22)$$

$$\frac{\partial T}{\partial A} = b \frac{\partial T}{\partial z}, \quad z=0 \quad (23)$$

Equations (22), (23) together with the initial and boundary conditions can be solved by the method of Laplace Transform. The result is

$$T(r, z, t) = T_f - (T_f - T_i) \operatorname{erfc} \left( \frac{\pi b r^2 + z}{2(at)^{\frac{1}{2}}} \right) \quad (24)$$

Where  $\operatorname{erfc}$  denotes the complementary error function which is tabulated in the mathematical literature (Carslaw and Jaeger, 1959, p. 485).

Typical well data are tabulated in Table 4.

Table 4. Well and Fluid Properties for a Borehole-Fracture System

---

a	Thermal diffusivity of the rock, $m^2/sec$	$10^{-6}$
c	Specific heat of the rock, $kJ/kg-^{\circ}C$	1
k	Heat conductivity of the rock, $kJ/m-^{\circ}C-sec$	$3 \times 10^{-3}$
q	Flow rate of the fluid, $kg/sec$	10
s	Specific heat of the fluid, $kJ/kg-^{\circ}C$	4
$T_i$	Initial temperature of the fluid, $^{\circ}C$	10
$T_f$	Temperature of the rock formation, $^{\circ}C$	110
$\rho$	Density of the rock, $kg/m^3$	$3 \times 10^3$
$\rho_w$	Density of the fluid, $kg/m^3$	$10^3$

---

Let  $z=0$ . Equation (24) gives the temperature distribution as a function of time and distance from the fracture

$$T(r,0,t) = T_f - (T_f - T_i) \operatorname{erfc}\left(\frac{\pi b r^2}{2(at)^{\frac{1}{2}}}\right) \quad (25)$$

Figure 11 gives the temperature distribution along the fracture in the radial direction after one month of the fluid invasion. Under the constant flow rate of 10 kg/sec, the fracture remains almost undisturbed at a distance of 120 meters away from the fracture. Figure 12 shows the temperature distribution at a distance of 100 meters away as a function of time. A whole year is needed for the fracture to cool down to 55°C at this distance.

#### Temperature Disturbance Resulting from Drilling Fluid Loss

The results of the preceding section will now be used to find the temperature disturbance due to the drilling process. Letting  $r=0$  in equation (24), the temperature at the borehole at time  $t_0$  is

$$T(0,z,t_0) = T_f - (T_f - T_i) \operatorname{erfc}\left(\frac{z}{2(at_0)^{\frac{1}{2}}}\right)$$

$T(0,z,t_0)$  is depicted in Figure 13. An obvious temperature inversion can be found in the vicinity of the fracture.

It is of interest to find a distance from the fracture

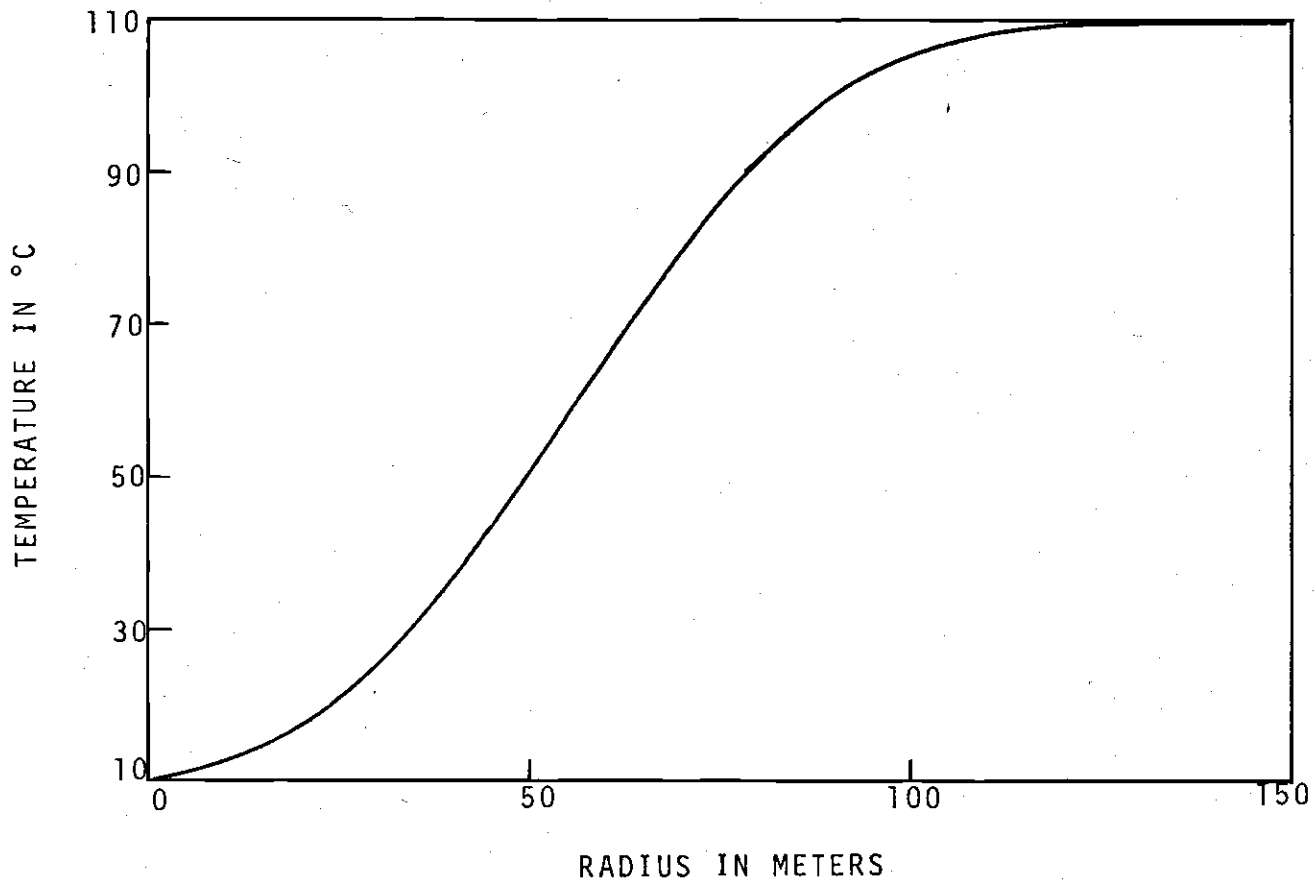


Figure 11. Temperature Distribution in the Fracture after One Month.

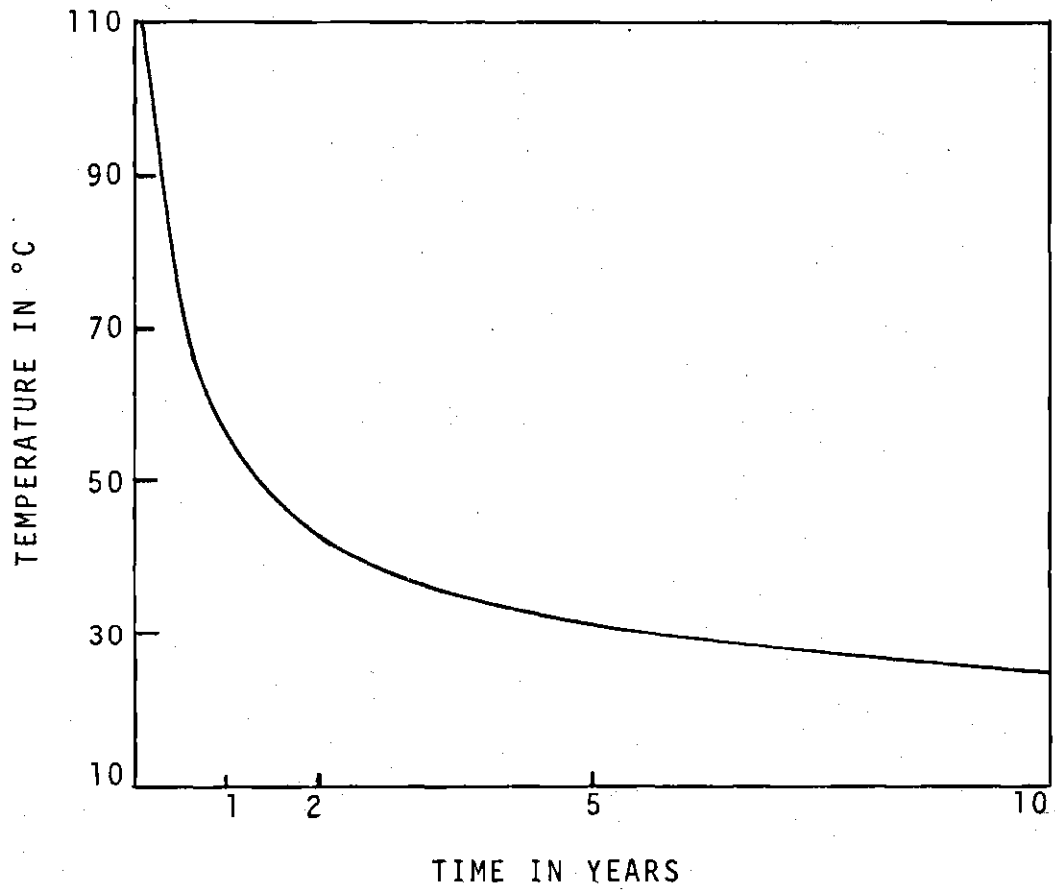


Figure 12. Temperature Distribution in the Fracture at 100 Meters away from the Borehole.

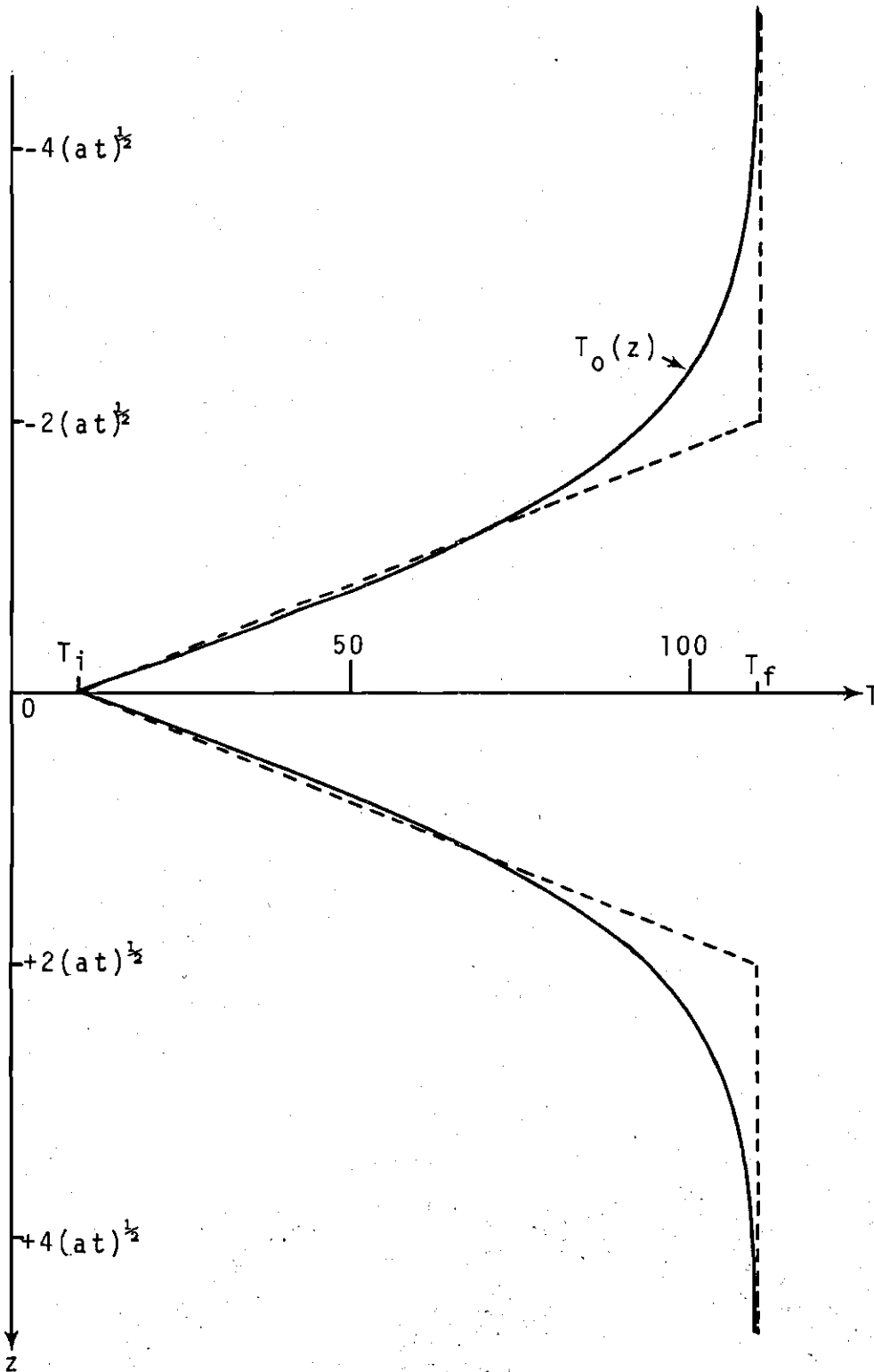


Figure 13. Temperature Disturbance in the Vicinity of a Fracture. Broken Lines are the Line Segments Approximate to  $T_0(z)$ .



beyond which only negligible effect can be detected. Noting that  $\text{erfc}(2) < .005$ , then such a distance would be estimated by  $T_0(z_m) \doteq T_f$  if  $z_m$  were selected such that  $(z_m/2(at_0)^{1/2}) \geq 2$ . Thus  $z_m$  represents the minimum distance from the fracture such that beyond  $z_m$  the temperature disturbance can be neglected.

$$z_m/2(at_0)^{1/2} = 2$$

$$z_m = 4(at_0)^{1/2}$$

$z_m = 6.4$  meters if  $t_0$  is one month (approximately  $2.5 \times 10^6$  seconds). The perturbation near the borehole exists in a region roughly 13 meters wide. Since measurements are often made at intervals of 10 meters or greater, it may be possible to miss the perturbation. If a continuous temperature log were taken, it may be observed.

#### Relaxation after the Drilling Ceases

It is of some interest to see how long it would take for the perturbation to dissipate by heat conduction. Assume the drilling process ceases at time  $t=t_0$ . The initial temperature distribution at the borehole will be  $T_0(z)$ .

$$T_0(z) = T_f - (T_f - T_i) \text{erfc}\left(\frac{z}{2(at_0)^{1/2}}\right), \quad t=0$$

To solve the heat conduction equation with the initial condition shown above is difficult; however, an approximation method is possible. Figure 13 shows  $T_0(z)$  can be approximated by four straight line segments.

$$\begin{aligned}
 T_0(z) &= T_f & z \leq -D & & (26) \\
 &= T_f - (T_f - T_i)(1 + z/D) & -D \leq z \leq 0 \\
 &= T_f - (T_f - T_i)(1 - z/D) & 0 \leq z \leq D \\
 &= T_f & D \leq z
 \end{aligned}$$

where  $D = 2(at_0)^{1/2}$

The Green's function method is appropriate (Carslaw and Jaeger, 1959) and the solution is

$$\begin{aligned}
 T(z, t) &= T_f - \frac{1}{2}(T_f - T_i) \left( \operatorname{erf}\left(\frac{D+z}{2(at)^{1/2}}\right) - \operatorname{erf}\left(\frac{D-z}{2(at)^{1/2}}\right) \right) \\
 &\quad - \frac{1}{2}(T_f - T_i) \left( \frac{z}{D} \right) \left( \operatorname{erf}\left(\frac{z+D}{2(at)^{1/2}}\right) + \operatorname{erf}\left(-\frac{z}{2(at)^{1/2}}\right) \right) \\
 &\quad - \operatorname{erf}\left(\frac{z}{2(at)^{1/2}}\right) - \operatorname{erf}\left(\frac{z-D}{2(at)^{1/2}}\right) + \left( \frac{T_f - T_i}{D} \right) (at/\pi)^{1/2} \\
 &\quad \left( \exp(-z^2/4at) - \exp(-(z+D)^2/4at) - \exp(-(z-D)^2/4at) \right) \\
 &\quad + \exp(-z^2/4at)
 \end{aligned}$$

At the fracture,  $z=0$

$$T(0,t) = T_f - (T_f - T_i) \operatorname{erf}(D/2(at)^{1/2}) + ((T_f - T_i)/D)(4at/\pi)^{1/2} \\ (1 - \exp(-D^2/4at))$$

Let  $D/2(at)^{1/2} = (t_0/t)^{1/2} = x$

Then

$$T(x) = T_f - (T_f - T_i) (\operatorname{erf}(x) - (1/\pi^{1/2}x)(1 - \exp(-x^2))) \quad (27)$$

Temperature versus time after the drilling ceases is depicted in Figure 14. If  $x=1/3$ , in other words 9 times the drilling period, the temperature in the borehole is still about  $18^\circ\text{C}$  away from equilibrium. This is much longer than the relaxation time estimated by Bullard (1947) in his conduction model. Thus the disturbance due to fluid invasion into the fracture is an effect not to be neglected.

#### Application of the Fluid-Loss Model

Figure 15 is a redrawing of the field data from a borehole (MG-16) in the Reykir geothermal area in Iceland. A measurement was made on February 25, 1973, 24 hours after the drilling stopped. An anomalous feature is observed between 650 and 850 meters deep. The measurement made approximately eight months later (October 18, 1973) reveals that the borehole had returned to equilibrium. A greater

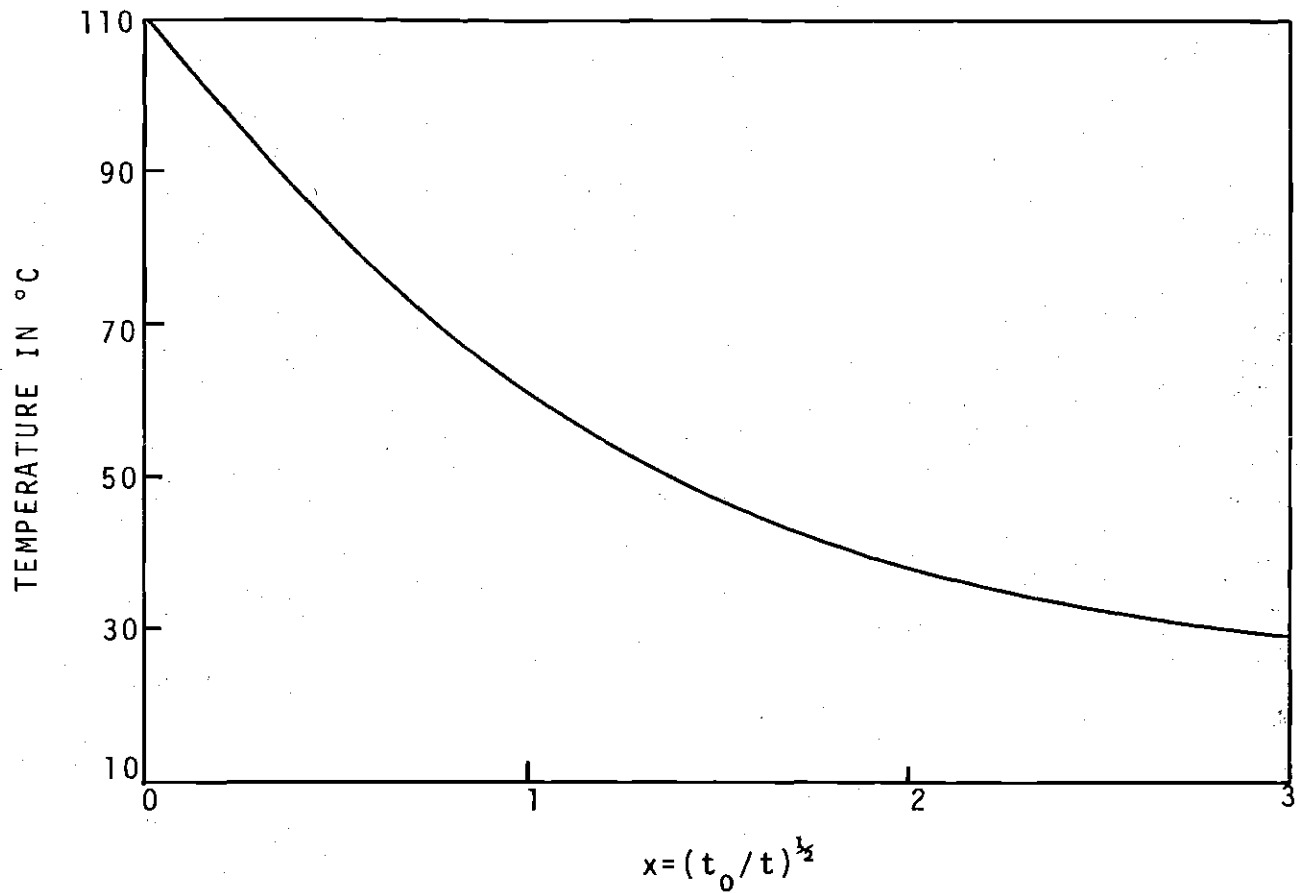


Figure 14. Temperature Vs. Relaxation Time.

## TEMPERATURE IN 10°C

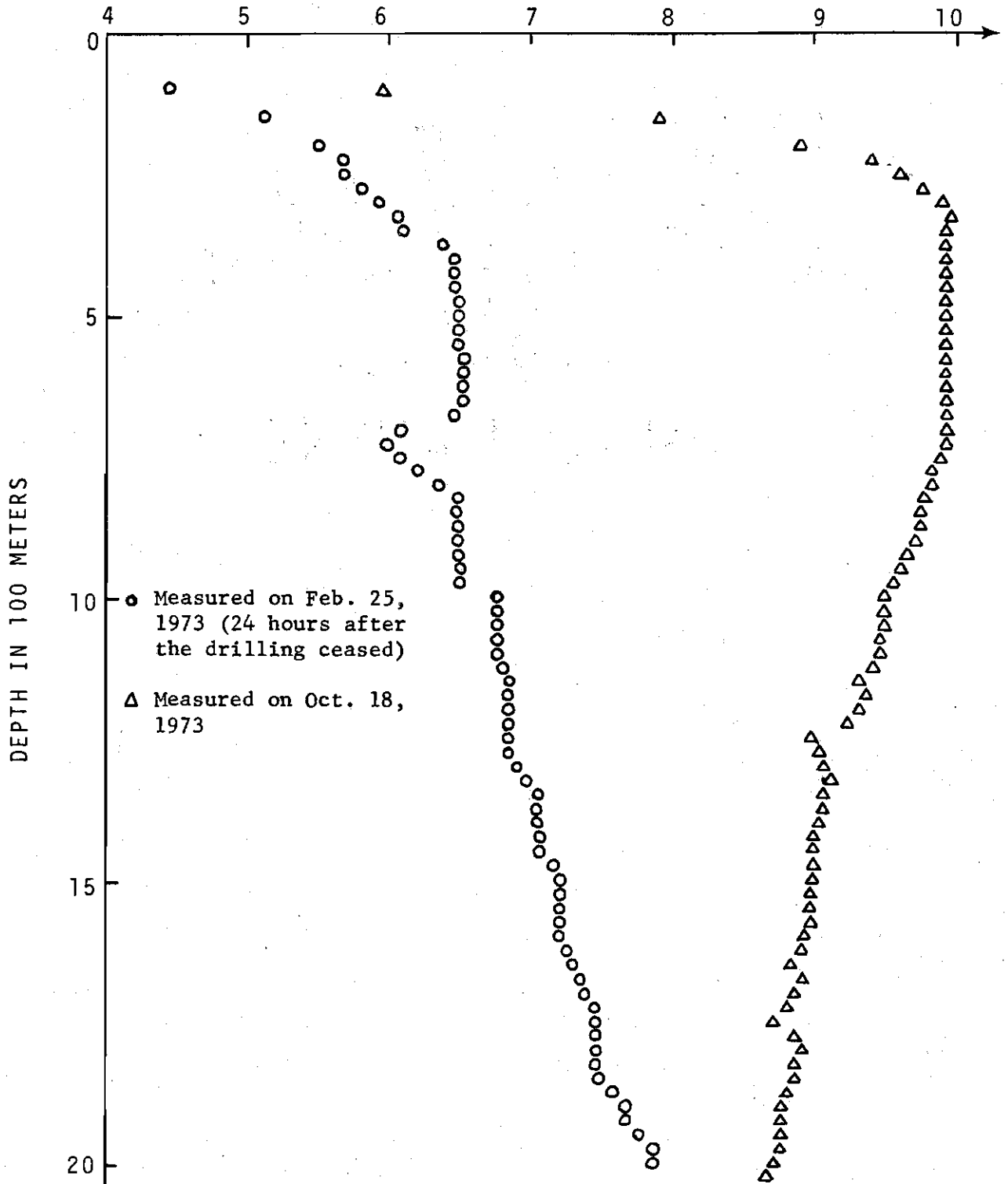


Figure 15. Temperature Data from a Borehole (MG-16) in the Reykir Geothermal Area (Courtesy of the National Energy Authority, Reykjavik, Iceland).

perturbation zone and shorter relaxation time are obtained than was estimated in the preceding sections. The large feature may be modeled by considering a number of parallel fractures. However, a more interesting problem is the relatively short relaxation time. It would seem that the conductive relaxation model may be inadequate. The rapid relaxation suggests that transient convection occurs in the fluid which has penetrated the formation. In order for convection to take place, the Rayleigh number must be greater than 40 (Lapwood, 1948). That is

$$R = \frac{K_p \alpha_o g \Delta T d}{(k / \rho_w c)} > 40 \quad (28)$$

where  $d$  = width of the fracture

$g$  = acceleration of gravity

$K_p$  = permeability of the rock

$\Delta T = T_f - T_i$

$\alpha_o$  = coefficient of thermal expansion

$\nu$  = viscosity of the fluid

Substituting into equation (28)  $\alpha_o = 2 \times 10^{-5} \text{ } 1/^\circ\text{C}$ ,  $g = 10 \text{ m/sec}^2$

$T = 100^\circ\text{C}$ ,  $d = 150 \text{ m}$ ,  $k = 3 \times 10^{-3} \text{ kJ/m-}^\circ\text{C-sec}$ ,  $\rho_w = 10^3 \text{ kg/m}^3$ ,  
 $c = 1 \text{ kJ/kg-}^\circ\text{C}$ ,  $\nu = 10^{-6} \text{ m}^2/\text{sec}$  leaves  $K_p$  as the only undefined parameter. For convection to occur, therefore,

$$K_p > 4 \times 10^{-11} \text{ m}^2$$

Thus a large zone of high permeability can provide a possible explanation for the observed features.

## CHAPTER IV

## CONCLUSIONS

The Jaeger (1961) and Holmes and Swift (1970) model provides a simple method for obtaining the steady-state temperature profile in the borehole and successfully predicts the bottom-hole temperatures. Since outlet temperature is so important, an approximation method is developed to make quick estimations of both  $T_{AO}$  and  $T_{BHT}$ . Calculations proved that the approximation method is good as long as  $H_1/H_2 > 20$ . To make use of the basic model in a geothermal area, some modifications are needed. The non-linear gradient system is used to model a geothermal borehole from Iceland. The fluid-loss model gives temperature profiles in the case when a portion of the drilling fluid is lost through fractures.

With the existence of fractures, the relaxation process is somewhat different from the normal situation. The temperature distribution of the fluid in the fracture is calculated. The temperature disturbance resulting from the drilling process gives an inversion feature similar to that of the observed temperature data (borehole MG-16). The relaxation time after the drilling ceases is also estimated. The long relaxation time illustrates that the disturbance due to fluid invasion can not be ignored. The fluid-loss model, however,



can not be applied directly to the available temperature data because the computed feature is so small that it can hardly be detected by standard temperature measuring techniques. Moreover, the rapid relaxation of the large temperature disturbance zone observed in Figure 15 suggests that the disturbance dissipates by means of thermal convection. The permeability of the rock formation in the geothermal production zone, in this case, must be greater than  $4 \times 10^{-11} \text{ m}^2$ . Such a high permeability is not unreasonable in fractured rocks.

## BIBLIOGRAPHY

- Bodvarsson, G., 1969, On the temperature of water flowing through fractures, J. Geophys. Res., 74, 1987-1992.
- Bodvarsson, G., 1970, Evaluation of geothermal prospects and the objectives of geothermal exploration, Geoexploration, 8, 7-11.
- Bodvarsson, G., 1972, Thermal problems in the siting of reinjection wells, Geothermics, 1, 63-66.
- Bodvarsson, G., 1973, Thermal inversions in geothermal systems, Geoexploration, 11, 141-149.
- Bullard, E. C., 1947, The time necessary for a borehole to attain temperature equilibrium, Monthly Notices Roy. Astron. Soc. Geophysics Suppl., 5, 127-130.
- Carslaw, H. S. and J. C. Jaeger, 1959, Conduction of heat in solids, 2nd ed., Oxford, Clarendon Press, 510 p.
- Holmes, C. S. and S. C. Swift, 1970. Calculations of circulating mud temperatures, J. Pet. Tech., 22, 670-674.
- Jaeger, J. C., 1961, The effect of the drilling fluid on temperatures measured in boreholes, J. Geophys. Res., 66, 563-569.
- Lachenbruch, A. H. and M. C. Brewer, 1959, Dissipation of the temperature effect of drilling a well Arctic Alaska, U. S. Geol. Survey Bull., 1083-C, 73-109.
- Lapwood, E. R., 1948, Convection of a fluid in a porous medium, Proc. Cambridge Phil. Soc., 44, 508-521.
- Keller, H. H., E. J. Couch, and P. M. Berry, 1973, Temperature distribution in circulating mud columns, Soc. Pet. Eng. J., 13, 23-30.
- Raymond, L. R., 1969, Temperature distribution in a circulating drilling fluid, J. Pet. Tech., 21, 333-341.
- Sigurmundsson, S., 1967, Temperature measurements in boreholes, 1966, Internal Report, National Energy Authority, Reykjavik, 12 pp.